Available online at www.sciencedirect.com
SCIENCE DIRECT
Polymer 45 (2004) 7615–7625
polymer
www.elsevier.com/locate/polymer

The properties of poly(tetrafluoroethylene) (PTFE) in compression

P.J. Rae[a,*], D.M. Dattelbaum[b]

[a]Los Alamos National Laboratory, Structure Property Relations, MST-8, MS-G755, Los Alamos, NM 85745, USA
[b]Los Alamos National Laboratory, Materials Dynamics, DX-2, MS-P952, Los Alamos, NM 85745, USA

Received 1 March 2004; received in revised form 23 August 2004; accepted 30 August 2004
Available online 15 September 2004

Abstract

Samples of DuPont 7A and 7C Teflon (PTFE, poly(tetrafluoroethylene)) were tested in compression at strain-rates between 10^{-4} and 1 s^{-1} and temperatures between −198 and 200 °C. Additionally, using a Split-Hopkinson pressure bar, a temperature compression series was undertaken between −100 and 150 °C at a strain rate of 3200 s^{-1}. To investigate the small-strain response, strain gauges were used to measure axial and transverse strain allowing the Poisson ratio to be quantified. As expected, the mechanical properties were found to be strongly affected by strain-rate and temperature. Moduli were found by several methods and the trend, with respect to temperature, lends weight to the suggestion that the glass-transition temperature of PTFE is ≈ −100 °C. The physical properties of the sintered PTFE were measured and the crystallinities measured by several techniques.

PACS: 62.20.Dc; 81.05.Lg; 85.35.Lr

Keywords: Polytetrafluoroethylene; PTFE; Compression

1. Introduction

Polymers are commonly used in manufacture and engineering, however, published research describing their mechanical properties is seemingly underrepresented given their importance. Much of the data that is presented, all too commonly gives insufficient information about the exact pedigree of the polymer tested and its processing history. This is possibly because establishing the base-line material characterisation is often as difficult as performing the actual mechanical tests. Additionally, accurate computer modelling of polymer mechanical response is still in its infancy. Many empirical methods are commonly employed, but they tend to be inaccurate outside of a narrow parameter range [1,2]. One reason for this, aside from the complexity of polymer response, is that often data is unavailable outside of a narrow experimental parameter range to challenge and expand the robustness of empirical or phenomenological based constitutive models. Here, we present the first results of a concerted multi-disciplinary effort aimed at understanding the mechanical response of a well characterised polymer from both an experimental view point and later, coupled with the production of a robust theoretical model capable of being implemented into computer codes.

The polymer described in this study is poly(tetrafluoroethylene) (PTFE). It was chosen for several reasons, including its use as a common engineering material for small high-performance parts and its availability from several manufacturers. While studied extensively in the past, it has received little attention in the open literature for the last 25 years. We have chosen to revisit this material because of its structural complexity and lack of mechanical data. PTFE is a remarkable material in many ways [3,4]. It exhibits useful properties over the widest temperature range of any polymer; PTFE retains some measure of ductility at 4 K and in some situations is used in applications at 540 °C. It is insoluble in all common solvents and is resistant to almost all acidic and caustic materials. PTFE has amongst the highest resistivity of any material, a very high dielectric

* Corresponding author. Tel.: +1-505-667-4436; fax: +1-505-667-8021.
E-mail addresses: prae@lanl.gov (P.J. Rae), danadat@lanl.gov (D.M. Dattelbaum).

0032-3861/$ - see front matter © 2004 Elsevier Ltd. All rights reserved.
doi:10.1016/j.polymer.2004.08.064

strength and low dielectric loss. The coefficient of sliding friction between PTFE and many engineering materials is extremely low and when sintered with wear reducing compounds, an industrially important class of bearing materials are formed. Coupled to its low coefficient of friction and chemical stability, PTFE is almost impossible for other materials to adhere to. This property is often used in industrial processing technology where ease of cleaning is important. One aspect of PTFE that has held it back from more extensive industrial and engineering use is its high melt viscosity (10^{11} P at 380 °C). This prevents injection and blow moulding from being possible and only expensive sintering and extrusion manufacturing processes are available for part production.

This paper focuses on base-line material characterisation and the compressive response of the pedigreed PTFE materials at differing strain-rates and temperatures. Future papers will deal with the tensile and shear response, detailed effects of polymer crystallinity, ballistic and shock behaviour and the development of an applicable theoretical constitutive model.

Very little previous research on the compressive properties of PTFE has been published. Some research on the creep properties exists [5–8], but in terms of engineering deformation, only six references have come to the attention of the authors. In 1963, Davies published a paper on the development of a Split-Hopkinson bar system. As part of this report, a single room temperature stress/strain curve for PTFE was presented at $\approx 1700\ s^{-1}$ [9]. The maximum strain imposed in this system was only 3%. Further high-strain rate data on Teflon versus temperature was published by Gray [10] and Walley [11]. Koo published stress/strain data for an Imperial Chemical Industries PTFE product called Halon G-80 in 1965 [12]. The effects of temperature on the mechanical response were also briefly discussed. DuPont has published a guide to material properties that contains three compression curves at 23, 100 and 204 °C to approximately 25% strain [13]. Finally, in 2001, Khan published some room temperature strain-rate sensitivity data for PTFE between 10^{-4} and 1 s^{-1} [14].

2. Materials

$600 \times 600 \times 65\ mm^3$ square billets of poly(tetrafluoroethylene) were prepared by Balfor Industries according to the ASTM standard ASTM-D-4894-98a by sintering and pressing poly(tetrafluoroethylene) molding powders (DuPont PTFE 7A and DuPont PTFE 7C). Billets were molded at 2500 (7A) and 2000 (7C) psi.[1] Both materials were heated to a 300 °C 6 h soak temperature at 36 °C h^{-1} before a 6 h melt at 357 °C. The cooling rate was continuous at 36 °C h^{-1}.

PTFE is somewhat unusual in having an as-polymerised melt temperature of ≈341 °C while the subsequent melting temperature is ≈328 °C. The billets were sampled regionally to test for homogeneity. The 7A PTFE billet was found to have only partially sintered molding powder at its centre[2] evidenced by a double melt endotherm (≈328 and 341 °C) in the modulated differential scanning calorimetry (MDSC) traces. Consequently, samples from this region were excluded from this study. Prior to commencing our research, trial compression samples were machined from 3 billet orientations, including a through-thickness series to establish if the material was isotropic. No statistical differences were discovered, except from samples taken near the billet skin, where a 5% increase in compressive yield strength was found. For this reason, compression samples used for tests were not machined from the skin region (i.e. a region within 5 mm of a surface).

PTFE is a semi-crystalline polymer. The crystalline percentage may be altered for a given molecular weight by altering the heat treatment profile used in production (thermal history). Several methods were employed to determine the crystallinity percentage of our example materials. These include infra-red spectroscopy, MDSC, density measurements and wide-angle X-ray scattering (WAXS). After completing the initial base-line characterisation, several interesting aspects of the response were difficult to explain without a brief investigation of the amorphous and crystalline regions response to temperature. For this reason, samples of 7C Teflon were thermally treated to alter crystallinity and compression samples machined and tested. Details of this process are presented later.

Poly(tetrafluoroethylene) exists in at least 4 known phases depending on pressure and temperature. Fig. 1 shows a schematic of these states. This plot is for illustrative purposes only and the exact pressure dependencies are not thought to be totally correct (see for example Refs. [15–18] for four different estimates of the phase II to III pressure induced phase transition). Further work at LANL is underway to better quantify the phase diagram at higher pressures.

The three relaxations of PTFE at atmospheric pressure have been investigated by McCrum [19] and are shown in Fig. 2. The broad peak centered at 20 °C represents a first order phase transition whilst the α and γ peaks are second order.

2.1. Infrared spectroscopy

Infrared spectroscopy was used to determine crystallinity percentage by a method described by Moynihan [20]. The percentage of amorphous material ($\%A_m$) is determined by

[1] The pressing cycle was as follows: Teflon 7A, 0–2500 psi (30 min), hold at 2500 psi for 15 min, 2500–0 psi (15 min). For Teflon 7C, 0–2000 psi (30 min), hold at 2000 psi (15 min), 2000–0 psi (15 min).

[2] A band in the centre approximately 8 mm thick.

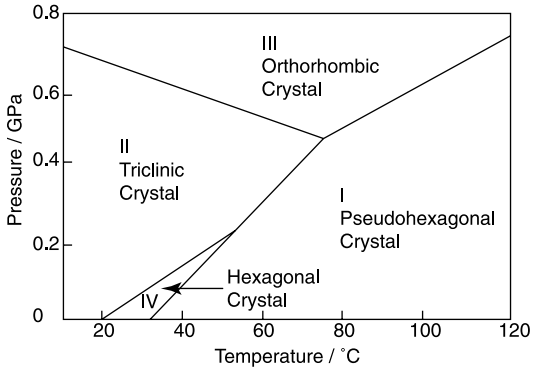

Fig. 1. Schematic of the phase diagram of PTFE at low pressures.

the ratio of the intensity of two bands in the mid-infrared at 778 and 2353 cm^{-1} and the relation,

$$\%A_m = 30.26\frac{A_{778}}{A_{2353}} + 1.73\left(\frac{A_{778}}{A_{2353}}\right)^2 \quad (1)$$

PTFE samples were microtomed at room temperature to a thickness of 500 nm and placed on dry KBr pellets (13 × 2 mm^2 discs). Spectra were taken in transmission mode using a Spectra-Tech Research Plan microscope coupled to a Nicolet SXB20 infrared spectrometer with mercury cadmium telluride detection. Sample data were collected in blocks of 256 scans at 4 cm^{-1} resolution. Baseline correction and band integration were performed using the Galactic Grams 32 AI software package according to the user instructions. The same frequency points were used for baseline correction in all data files and the results are reported in Table 1. The greatest challenge with this technique is the baseline correction procedure. Only small absorption peaks are present at the wave-numbers of interest see, see Fig. 3, leading to potentially large errors in the measured crystallinity. Moynihan used much thicker samples and may have saturated the detector at the strong CF_2 stretching absorptions near 1200 cm^{-1} invalidating an assumed linear response in Beer's law. Finally, to the authors knowledge, no research has been published on the orientation or crystallinity changing effects of microtoming the test samples for this type of procedure. Lehnert's [21]

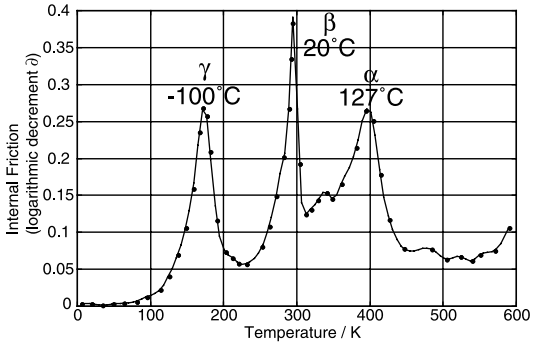

Fig. 2. Relaxations of PTFE (partially redrawn from Ref. [19]).

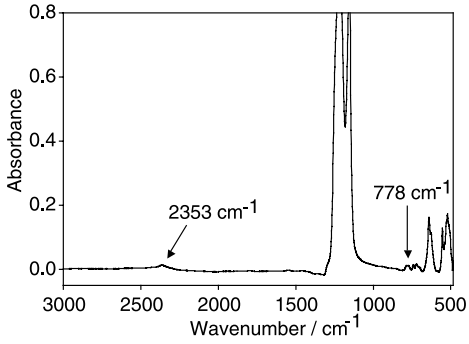

Fig. 3. The mid-infrared absorption curve of PTFE.

estimation of the error in this technique is approximately 10% compared to the reported error by Moynihan of 1%.

2.2. Modulated differential scanning calorimetry

Thermal properties were measured using a TA Instruments 2920 modulated differential scanning calorimeter Samples (ca. 10 mg) were loaded and sealed in standard DSC pans, and cooled to −145 °C. They were scanned at a rate of 2.0 °C min^{-1} with a modulation of ±1.0 °C every 60 s to 400 °C under a nitrogen purge. The MDSC was used to verify literature values for ambient pressure phase transitions and determine the melting temperature (T_m). Crystal–crystal transitions at 19 and 30 °C were evident in the MDSC trace together with a melt transition at 327.5 °C. The percentage of crystallinity can be estimated by integrating the melt endotherm (heat of fusion) and calculating the ratio with a theoretical 100% crystalline sample. Values for the heat of fusion (ΔH_f^0) for PTFE in the literature range from 57 to 104 J g^{-1} [21]. For our calculations, we used a value of 80 J g^{-1} and calculated the weight fraction crystallinity by the relation $X_c = \Delta H_f$ (sample)/ΔH_f^0.

2.3. Density measurements

Density measurements were performed using two methods: immersion in ethanol and helium gas pycnometry (Micromeritics Accupyc 1330). Both methods are based on volume displacement (either with liquid or gas) and sample mass. There was good correlation between the two methods indicating insignificant void content in the billet samples. The density values were used to estimate the volume fraction crystallinity (ϕ_c) using the following relation,

$$\phi_c = \frac{(\rho - \rho_a)}{(\rho_c - \rho_a)} \quad (2)$$

where ρ is the sample density, ρ_a is the extrapolated density of the pure amorphous phase ($\approx 2040 \pm 30$ kg m^{-3}) and ρ_c is the extrapolated density of the pure crystalline phase ($\approx 2300 \pm 10$ kg m^{-3}) [3,21]. The densities of the pure amorphous and crystalline phases must be estimated from

Table 1
Measured mass fraction crystallinities of the PTFE materials by different methods

Material	Density (kg m^{-3})	IR (% xstal)	Density (% xstal)	MDSC (% xstal)	WAXS (% xstal)
7A Teflon	2157.7±0.1[a] 2158.3±0.1[b]	73±10	43±1	38±1	69±2
7C Teflon	2168.9±0.1[a] 2169.6±0.1[b]	N/A	48±1	38±1	69±2

[a] Pycnometry.
[b] Immersion.

extrapolation because PTFE cannot be manufactured in one exclusive phase.

The volume fraction can be converted to a mass fraction (X_c) for comparison to other methods by the relation $\phi_c = (\rho/\rho_c)X_c$. These results are also summarised in Table 1.

2.4. Wide-angle X-ray scattering

Unit cell structures and crystallinities were determined from a θ to 2θ X-ray diffraction pattern. A Rigaku ROTAFLEX RTP300 rotating anode X-ray generator with a Cu target and a Ni filter produced Cu K_α ($\lambda = 0.154$ nm) X-rays. The goniometer was calibrated with NaCl to within 0.5°. The samples were continuously scanned from 4 to 50° at a rate of 1 deg min^{-1} and the data were analyzed according to a method described by Ryland [22]. A typical trace for Teflon 7C is shown in Fig. 4. The crystalline (110) peak and its amorphous halo were both integrated (I_c, I_a) in 2-Theta space using the Galactic Grams 32 AI spectral analysis software. From these integrated peak areas, the ratio X_c/X_a can be calculated by $X_c/X_a = 1.8(I_c/I_a)$ Ryland's factor of 1.8 is commonly used for semi-crystalline polymers. It is not well-defined and being a simple scalar can greatly affect the resulting value. The percentage crystallinity is obtained from $X_c\ (\%) = 100 - 100/(1 + X_c/X_a)$.

2.5. Thermally treated 7C material

In order to understand some of the compression test data on 7A and 7C, production of some PTFE with differing levels of crystallinity was useful. It was found that thermally treating 7C Teflon produced a 3–4% wider variation in crystallinity than 7A and so this material was exclusively used for production of compression samples.

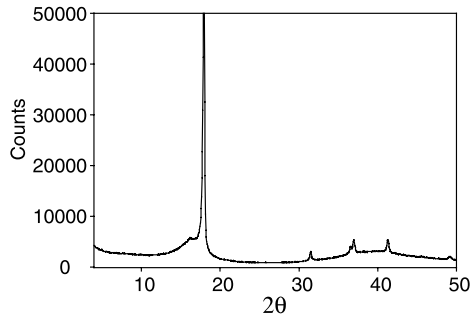

Fig. 4. A typical Teflon 7C WAXS trace showing a strong crystalline peak superposed over an amorphous halo.

Bars of 7C $12\times12\times65$ mm^3 were rough sawn for processing. To produce high crystallinity material, samples were heated to 350 °C and cooled at an average rate of 1.75 °C h^{-1} until 280 °C. For the production of lower crystallinity samples, quenching in ice–water from 350 °C was tried but found to produce inhomogeneous material. Regions of higher and lower crystallinity could be seen as translucent and more opaque regions about 15 mm^3 in size. Upon attempting compression tests on samples machined from these bars, inhomogeneous deformation resulted from the harder and softer regions. Uniform lower crystallinity material was produced by rapid ambient air cooling after a 5 h soak at 380 °C. Table 2 shows the resulting crystallinities.

A variation in crystallinity of 11–16% may not seem impressive compared to the studies of Thomas, McCrum and Moynihan [19,20,23] that involved crystallinities from ca. 40 to 95%, however closer examination shows that in these studies differing molecular weight PTFE moulding powder was used to access this wide variation. For our study, it was felt important to maintain the same molecular weight material throughout.

3. Experimental

Given the ductile nature of PTFE, the mechanical properties were investigated at both large and small strains. For this reason, all strains referenced in this paper are true-strains (logarithmic strains). Additionally, a constant loading strain-rate was maintained for all large-strain experiments. The feedback loop from the testing machines was closed to correctly slow the crosshead as the samples thinned. In large-strain experiments, true-stress was calculated assuming a constant sample volume. This volume assumption will later be shown to be true for strains greater than approximately 5%.

Table 2
Measured mass fraction crystallinities of the thermally treated 7C

Material	Density (kg m^{-3})	Density (% xstal)	MDSC (% xstal)
Low crystallinity	2154.4±0.1[a]	47±1	32±1
High crystallinity	2182.9±0.1[a]	58±1	48±1

[a] Pycnometry.

The sample geometry chosen was 6.375 mm diameter by 6.375 mm long right-regular cylinders. The aspect ratio of 1:1 is smaller than the 1:1.5–1:2 values often employed in compression tests on metals. Various other geometries were tried, but it was discovered that samples with ratios of $\approx$1:1.5 or higher tended to deform by a mixture of shearing and compression rather than by uniaxial compression. The sample size and ratio was therefore chosen to conserve material for the large number of tests required and ensure that the test was purely compressive. In view of the naturally low coefficient of friction for PTFE against most materials and the experimental steps described later, minimal sample barreling occurred even when deformed to 50% true-strain.

For low strain-rate experiments ($<0.01\ s^{-1}$), a screw driven Instron 1125 frame was used. This machine has been upgraded with a modern PC control system (MTS Testworks 4[3]) allowing a wide range of control modes and input channels. For strain rates between 0.01 and $1\ s^{-1}$ a MTS 880 servo-hydraulic machine was utilized. This machine ran MTS TestStar software also allowing for full control over the test profile. In all samples tested at -20 °C, or higher, paraffin wax was used to lubricate the specimen ends [24,25]. The specimens were compressed between highly polished tungsten carbide platens to further lower the friction. Temperature control was carried out using either electrically heated or liquid nitrogen cooled platens and surrounding insulation was used to create a small environmental chamber. The samples were allowed to equilibrate at temperature for between 45 and 100 min prior to testing.

In the large-strain compression experiments, linear variable displacement transformer and single arm displacement gauges were used to measure the sample deformation. These techniques are not suitable for small strains (<0.02) and so strain gauges were bonded to larger 7A and 7C samples to obtain low-strain data. Normally, adhesives do not adhere to PTFE, however, the surface of the samples was etched with a sodium-based commercial product by ABB Etching,[4] Arizona, USA resulting in surface removal of fluorine atoms and the subsequent replacement with OH groups when exposed to water vapour in the atmosphere. After etching, strain-gauge quality cyano-acrylate adhesive could be used to bond Measurements Group, USA, CEA-06-062WT-120 gauges to samples 19 mm in diameter and 38 mm tall. These gauges have two active directions allowing axial and transverse strain to be measured simultaneously. In this way, the Poisson ratio at small strains could be calculated. The measured noise on the strain gauge signals was approximately 24 $\mu\varepsilon$ rms in an experiment that was run out to 20 millistrain. Because a ratio is taken for the Poisson value and nominally identical gauges are used in each orientation, to a first order, any systematic errors are cancelled.

For high strain-rate testing ($3200\ s^{-1}$), a LANL-built Split-pressure Hopkinson bar was used [26]. This Hopkinson bar is fitted with a small environmental chamber surrounding the test sample. In the chamber, either heated or cooled gas can be introduced to vary the sample temperature between -100 and $+150$ °C. The change in impedance at the ends of the Ti-6Al-4V bars used for testing in this temperature range is negligible. As before, paraffin wax was used to lubricate the specimen ends for all samples tested at -20 °C or higher. No lubricant was used at lower temperatures, but owing to the relatively small strains imposed on the sample and the low coefficient of friction between PTFE and the finely finished pressure bars, no sample barreling was found.

The speed of sound in the Teflon materials was measured using a time of flight method [27]. Room temperature samples 58 mm thick were tested using longitudinal and shear wave inducing heads.[5] Suitably correcting for triggering and coupling medium delays, the results are shown in Table 3. Values for Young's modulus (E), Poisson ratio (ν) and shear modulus (G) are obtained using the material densities quoted in Table 1 and the following expressions,

$$\nu = \frac{C_l^2 - 2C_s^2}{2(C_l^2 - C_s^2)}, \tag{3}$$

$$E = 2\rho C_s^2(1+\nu), \tag{4}$$

$$G = \frac{E}{2(1+\nu)}, \tag{5}$$

where C_l and C_s are the longitudinal and shear wave-speeds, respectively, and ρ is the density. These expressions are only valid for isotropic solids within the elastic region, but given the minute strains induced by the ultrasonic transducers, this is a reasonable assumption. These sound speed values are comparable to those found by Perepechko, Marsh and Kaye although wide variation is evident between references[6] [28–30].

For computer modelling, it is important to know the fraction of work from deformation (strain) that is released as heat versus used internally to rearrange the structure. This is because the mechanical properties of polymers change significantly with modest temperature changes. When studying metals, this fraction is usually known as the beta-factor (β) and is typically >0.95, i.e. more than 95% of all plastic work put into a metallic specimen is released as heat [31]. The definition of the beta-factor is shown in Eq. (6), ρ is the density, c the specific heat capacity, T the temperature and σ and ε represent stress and strain, respectively. It has previously been reported that the beta-factor in glassy

[3] www.mts.com.
[4] www.abbetch.com.
[5] Panametrics 5077PR Pulser/Receiver, Panametrics V155 and V109 transducers. Timing obtained from a Tektronix TDS 754D Oscilloscope.
[6] C_l varies from 1230 to 1410 and C_s from 410 to 720 m s^{-1}.

Table 3
Ultrasonic wave-speeds and calculated elastic constants for Teflon 7A and 7C at 23 °C

Material	C_l (m s^{-1})	C_s (m s^{-1})	E (GPa)	ν	G (GPa)
7A Teflon	1307±3	503±2	1.5	0.41	0.55
7C Teflon	1333±3	506±2	1.6	0.42	0.56

polymers can be considerably lower than found in metals [32]. For this reason, an effort was made to measure the β factor in PTFE at modest strain-rates (10^{-1} s^{-1}).

$$\beta = \frac{\rho_c \Delta T}{\int \sigma_{ij} d\varepsilon_{ij}} \quad (6)$$

To determine the beta-factor, a 0.3 mm hole was drilled 3 mm deep into the side of standard PTFE compression. In-house constructed Type K thermocouples, 0.3 mm in diameter, were manufactured and inserted with a sliding fit into the samples. Once significant strain is applied (>5%) to the specimen, the thermocouple is in intimate contact with the sample centre. Data from the amplified thermocouple signal were logged by the MTS TestStar software coincident with the stress/strain data. For the β factor calculation, the measured immersion density was used and the specific heat capacity at just above room temperature estimated from Furukawa [33] (300 K, c=1100 J K^{-1} kg^{-1}).

4. Results

PTFE samples were tested at multiple strain-rates to quantify the material response. Figs. 5 and 6 show the experimental results. All samples were loaded to 50% true-strain without failure and the unloading curve (also undertaken in true strain-rate control) was also recorded. At least three samples were tested at each rate to probe reproducibility and a typical curve is plotted. Minimal sample-to-sample scatter was found. Samples of Teflon 7C exhibit a linear increase in yield stress and an increase in the rate of work-hardening with increasing rates from 1×10^{-4} to 1 s^{-1}. The 7A material displayed an aberration in this linear growth between 1×10^{-2} and 1×10^{-1} s^{-1}. It is believed that this aberration is a genuine material response because the experiment was repeated several times at these rates and gave reproducible results. At the other strain-rates, the response of the 7A and 7C materials was essentially identical. The samples all relaxed to approximately the same strain upon unloading, despite the significantly different loading and unloading strain-rates.

It is well known that temperature significantly affects the mechanical response of polymers [10,34]. Samples of PTFE were loaded to 50% true strain at temperatures between −198 and 200 °C. The results are plotted in Figs. 7 and 8. With the exception of the samples at −198 °C, the specimens did not fail and relaxed partially upon unloading. The samples tested at −198 °C all shattered at approximately 35% strain. This is a lower value than samples tested at higher strain rate by Walley [11]. His specimens failed at a true strain of 0.56 when cooled to approximately −173 °C. The large difference in strength of PTFE with temperature is evidenced by the logarithmic stress scale required to clearly present all the curves. No significant differences were found between the response of 7A and 7C Teflon as a function of temperature. As with the previous variable strain rate data, all the samples that survived to 50% strain recovered to approximately the same strain upon unloading.

To conclude, the strain-rate/temperature effect experiments, samples were deformed at 10^{-1} s^{-1} at several

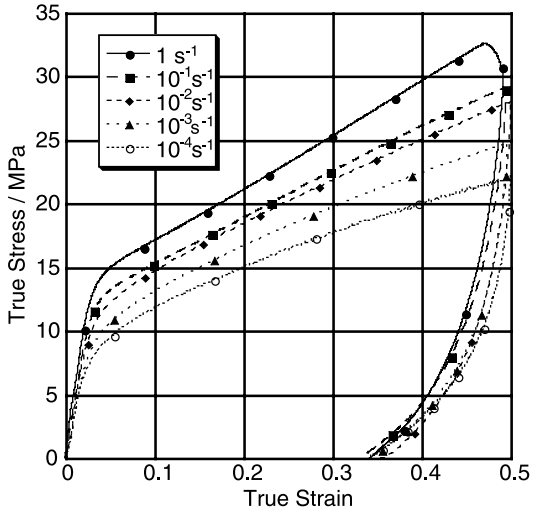

Fig. 5. Stress/strain curves for Teflon 7A at differing strain rates (26 °C).

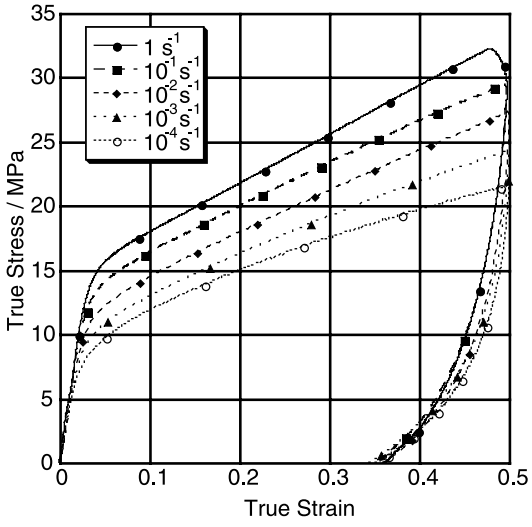

Fig. 6. Stress/strain curves for Teflon 7C at differing strain rates (26 °C).

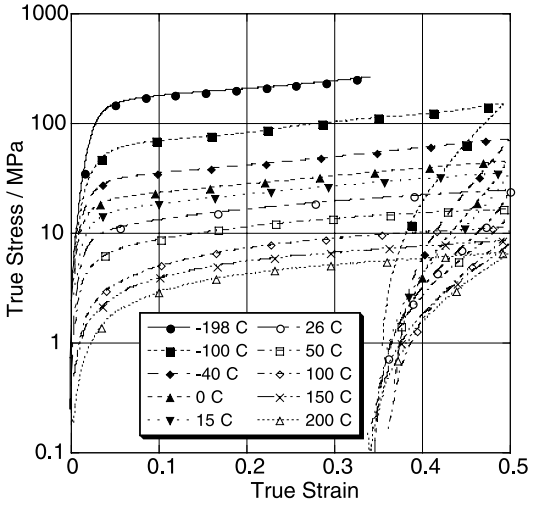

Fig. 7. Stress/strain curves for Teflon 7A over a wide temperature range ($10^{-3}\,s^{-1}$).

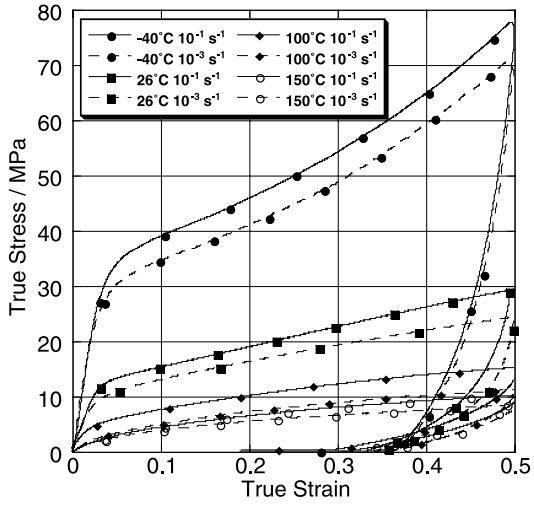

Fig. 9. Stress/strain curves for Teflon 7A over a wide temperature range and two strain-rates (10^{-3} and $10^{-1}\,s^{-1}$).

temperatures. In this way the superposition of rate and temperature can be compared with future model predictions. Figs. 9 and 10 show the results for 7A and 7C material, respectively, cross plotted with the appropriate $10^{-3}\,s^{-1}$ data already presented. As expected, deformation at higher rates still results in increased yield and flow stresses.

To better understand PTFE behaviour at higher strain-rates, a variable temperature series of tests was undertaken at $3200\,s^{-1}$, Figs. 11 and 12. All samples survived intact from these experiments although the strain imposed was significantly smaller that those used in the quasi-static load-frame experiments. Increasing the strain-rate from 1 to $3200\,s^{-1}$ resulted in an $\approx$50% increase in the flow stress at room temperature. The results for 7A and 7C materials are very similar except at $-100\,^{\circ}C$ where the 7A material displayed a slightly higher flow stress.

To investigate the flow stress of glassy PTFE, high and low crystallinity samples were tested at $-198\,^{\circ}C$ at a rate of $10^{-2}\,s^{-1}$. This was done by immersing the samples and platens in liquid nitrogen throughout testing. Fig. 13 shows the curves for differing crystallinities and the as-received 7C for reference. Interestingly, the low crystallinity material was able to be loaded to 50% true strain without failure, unlike the other samples that shattered. Clearly, at this temperature the glassy amorphous domains of PTFE are stronger and allow greater ductility than the crystalline regions. Additionally, stress/strain curves were recorded for the high and low crystallinity materials at 0, 24 and 50 °C to investigate the relative stiffness of the crystalline and amorphous domains. It was useful to establish if the temperature related strength of PTFE is more affected by the crystalline domains or the amorphous ones. Curves taken at 0 and 50 °C are presented in Figs. 14 and 15, respectively. To establish the crystallinity effect, a reproducible material parameter was required. Whilst a somewhat arbitrary measurement, an intersection of the initial

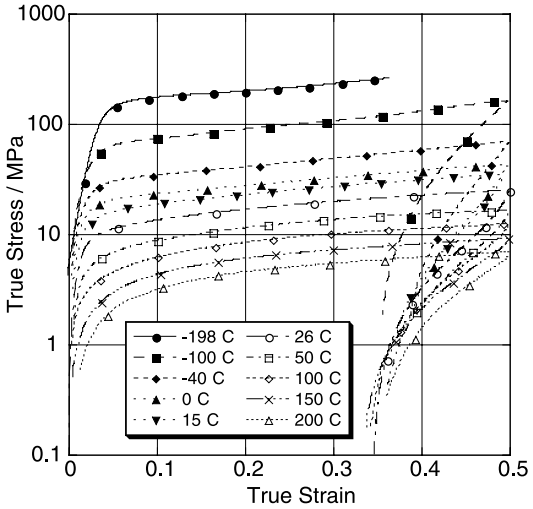

Fig. 8. Stress/strain curves for Teflon 7C over a wide temperature range ($10^{-3}\,s^{-1}$).

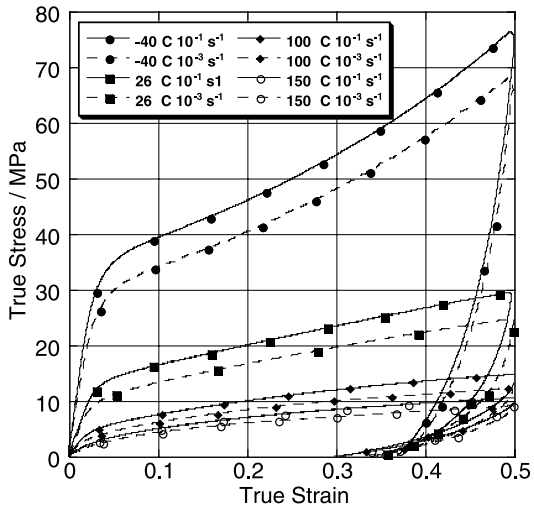

Fig. 10. Stress/strain curves for Teflon 7C over a wide temperature range and two strain-rates (10^{-3} and $10^{-1}\,s^{-1}$).

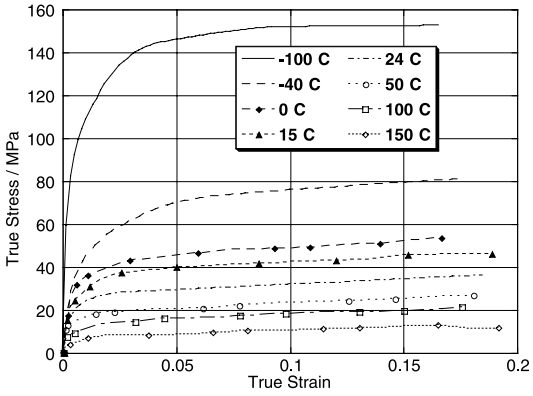

Fig. 11. Stress/strain curves for Teflon 7A at several temperatures ($3200 \pm 100\ s^{-1}$).

Table 4
The strength of variable crystallinity PTFE at 50, 24 and 0 °C

Temperature	Low crystallinity (MPa)	7C Teflon (MPa)	High crystallinity (MPa)
50	3.58	3.97	4.33
24	11.8	13.5	14.3
0	22.5	24.7	26.3
50/0 ratio	0.16	0.16	0.16

tangent modulus and a straight line fitted to the curve at 10 and 20% strain was chosen. In this way, a 'strength' was associated to each curve and the results are shown in Table 4. Given that the 50/0 ratio is constant, independent of PTFE crystallinity, suggests that around room temperature, and within the sensitivity of the experiment, the stress required to deform PTFE changes at the same rate in the crystalline and amorphous domains.

An estimate of the initial tangent modulus of 7A and 7C material was made with respect to temperature, Fig. 16. There has been some discussion about the glass transition temperature (T_g) in PTFE. Some researchers maintain that the α transition at 127 °C is also the glassy/amorphous transition T_g [19,35–37]; others maintain that it lies at the γ transition (−100 °C) [38–40]. Both are second-order

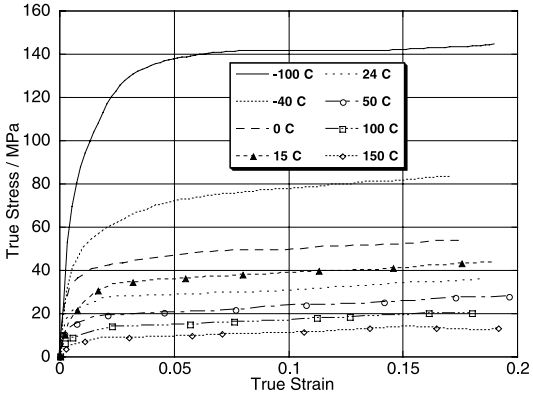

Fig. 12. Stress/strain curves for Teflon 7C at several temperatures ($3200 \pm 100\ s^{-1}$).

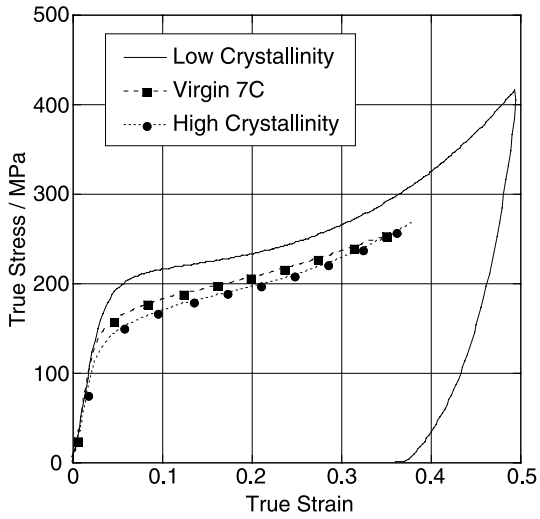

Fig. 13. Stress/strain plot of high and low crystallinity PTFE at −198 °C ($10^{-2}\ s^{-1}$).

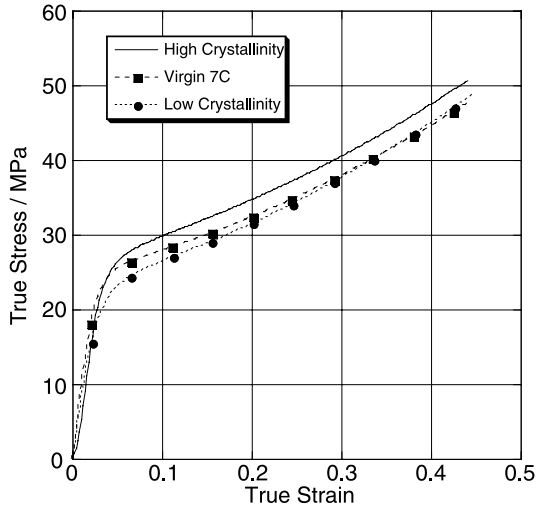

Fig. 14. High and low crystallinity PTFE stress/strain plot at 0 °C ($10^{-1}\ s^{-1}$).

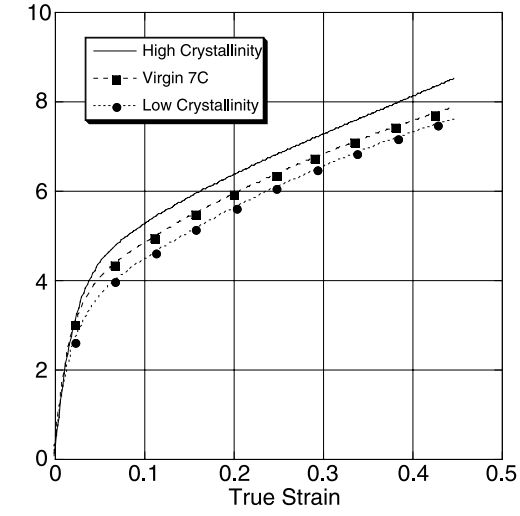

Fig. 15. High and low crystallinity PTFE stress/strain plot at 50 °C ($10^{-1}\ s^{-1}$).

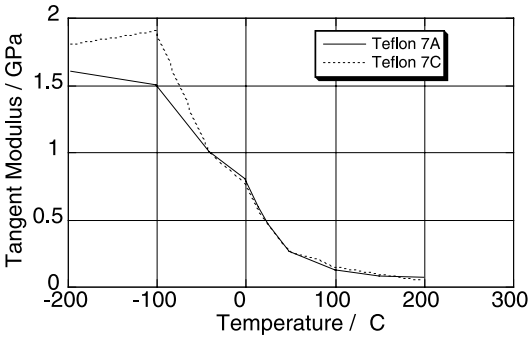

Fig. 16. Large-strain initial tangent modulus for Teflon 7A and 7C vs. temperature (10^{-3} s^{-1}).

transitions. One of the usual features present at a polymer T_g is an abrupt change in modulus. Fig. 16 lends weight to the argument that the true T_g for PTFE is coincident with the γ transition.

As explained previously, the methods used to measure strains in the previous curves were unsuitable for small deformations ($\varepsilon < 2\%$). Fig. 17 shows the room temperature stress/strain response of 7A and 7C material at low strains using strain gauges. At this resolution, the 7C material is slightly stiffer than the 7A. Taking initial tangent moduli gives 1.2 GPa for the 7C material and 1.0 GPa for 7A. Fig. 18 shows the corresponding Poisson ratio of the two PTFE materials. The ratio is fairly consistent at ≈ 0.47 over this strain range. Measurements made on samples subjected to strains larger than 5% indicate that to better than 1%, sample volume is conserved.

The β factor for Teflon 7A was measured as described previously. The temperature rise associated with the deformation of the samples was approximately 2.8 °C. This rise is too small to allow the sample to pass through the 30 °C phase transition. Fig. 19 shows that approximately $70 \pm 10\%$ of the work done on the sample was released as heat during loading to 50% true-strain.

5. Discussion

Each of the techniques for measuring crystallinity has caveats. Historically, the primary method for crystallinity determination in the literature is WAXS [22]. This technique, whilst reasonably straightforward in concept, has several associated problems. The scalar factor of 1.8 is introduced to correct for polarization, temperature and density effects, but little evidence was presented by Ryland to support the applicability of this factor with a range of polymers.[7] A second known problem with many PTFE billets of high-molecular, is a high degree of planer orientation at the billet surface (skin effect) formed during

[7] It is interesting to note that if the scalar factor were reduced to 1.0, the resulting crystallinity values are close to the values found by MDSC and density.

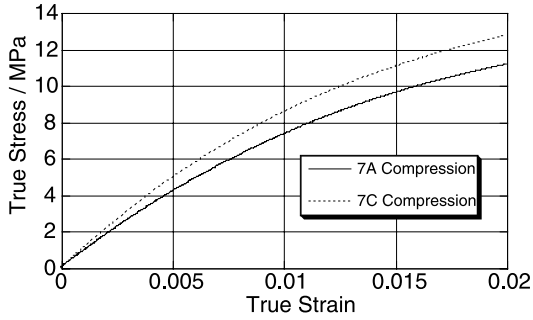

Fig. 17. Stress/strain plot for Teflon 7A and 7C ($\varepsilon < 0.02$, 26 °C).

manufacture. This molecular axis is parallel to specimen surface and is reflective in WAXS, thereby resulting in an over-estimation of the crystallinity [21]. Solutions to this problem include performing transmission WAXS on thin (ca. 1 mm) samples or machining the skin from test samples prior to measurement. This second option is rarely mentioned in the literature and might raise issues of surface finish effects. Nevertheless the samples used in our WAXS experiments were machined from the larger sintered billets.

MDSC uses heat of fusion of crystalline domains to determine X_c. A problem with this method is that ΔH_f is referenced to ΔH_f^0, a quantity that is experimentally unobtainable for PTFE. Teflon has a constantly changing structure as the temperature is raised higher than 30 °C (phase I). Determining over what range to determine ΔH_f^0 is problematic. The calculation also assumes a perfect two phase model (like other techniques) and therefore ignores regions of amorphous–crystalline transition zones and crystalline imperfection.

The density technique compares the actual sample density to those of a theoretical fully amorphous and fully crystalline sample of PTFE. Both of these are extrapolated values ($\rho_a \approx 2040$ and $\rho_c \approx 2300$ kg m^{-3}). As with MDSC, issues of amorphous–crystalline transition zones and crystalline perfection are ignored. Despite this, the density method of crystallinity estimation is perhaps the most accurate of the methods discussed here, provided that samples have negligible internal void content from insufficient pressing and thermal treatment.

As discussed by Lehnert, the crystallinity of our Teflon samples varied depending on the measurement method used

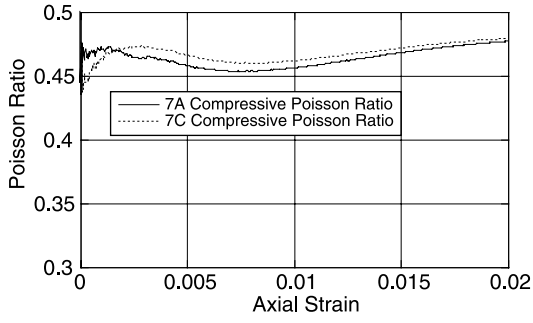

Fig. 18. Small-strain Poisson ratio for Teflon 7A and 7C (26 °C).

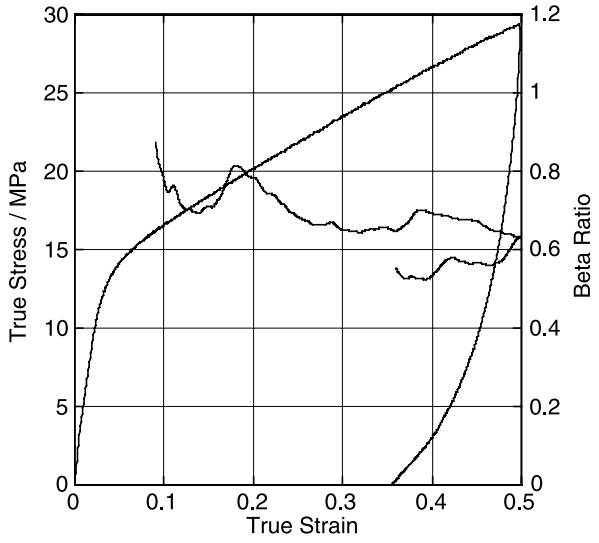

Fig. 19. Typical beta factor vs. strain curve for Teflon 7A at $10^{-1}\,s^{-1}$ and an initial temperature of 26 °C.

[21]. Typical literature values from other mechanical property studies were derived from WAXS data, however, in this study we prefer to reference the values derived from density measurements. From Table 1, it is clear that the 7C material was of slightly higher crystallinity than the 7A since all comparison techniques reflect this trend.

The longitudinal and shear wavespeeds were measured and are comparable with previously published data. Combining the density measurements allowed the Young's and shear modulus to be found together with the Poisson ratio. Comparison of the Young's modulus to initial tangent modulus, measured by strain gauges bonded to compression samples, showed the ultrasonic technique yielding 35% higher results. This is thought to be due to the lack of a linear elastic region in PTFE leading to a variable modulus that reduces with strain. The moduli measured at larger strains are considerably lower but possibly more representative of values required for engineering applications.

Table 4 compared the strengths of high and low crystallinity PTFE at three temperatures. A ratio was taken of the strength at 50 °C compared with 0 °C to see if the yield strength of crystalline domains was less affected by temperature than the amorphous ones. Within experimental error, whilst the crystalline region was always stronger, the rate of change with temperature was independent of the crystallinity. This is somewhat surprising given that the deformation mechanisms for amorphous chains are totally different to the slip and twinning response responsible for crystalline deformation.

In all cases, the Poisson ratio for PTFE was found to be greater than 0.4 with experiments showing a trend towards 0.5 at strains greater than 5%. It is not believed that the Poisson ratio values shown in Fig. 18 are valid below 0.2% owing to numerical instability in the calculation from random errors.

Little difference in the response of the materials with strain-rate or temperature can be observed except in the Hopkinson bar at −100 °C where the 7A material has a slightly higher flow stress. This may result from the slightly lower crystallinity found in the 7A Teflon and the fact that the amorphous domains are glassy at −100 °C.

During deformation, PTFE stores much more of the work done as structural change (≈30%) than typical metals (<10%). This energy is presumably used in crystallographic and amorphous chain rearrangement resulting in less sample heating than a comparable metal and therefore lowering the thermal softening effect of 'self' heating. This strain-induced rearrangement is partly temporary because polymers are viscoelastic and internal energy is expended during spring-back/relaxation or physical ageing.

Acknowledgements

The authors wish to thanks Dr Bruce Orler and Dr Rusty Gray for useful discussions regarding this research and Mike Lopez for advice on mechanical testing. This research was supported under the auspices of the US Department of Energy, specifically in part by the joint DoD/DoE Munitions Technology Development Program.

References

[1] Wortmann FJ. Modeling the dynamic performance of poly(tetrafluoroethylene) in the alpha-transition region. Polymer 1999;40:1611–5.
[2] Zerilli FJ, Armstrong RW. Thermal activation constituative model for polymers applied to polytetrafluoroethylene. In: Furnish MD, Thadhani NN, Horie Y, editors. Shock compression of condensed matter—2001. American Institute of Physics; 2001. p. 657–60.
[3] Sperati CA, Starkweather HW. Fluorine-containing polymers. ii. Polytetrafluoroethylene. Adv Polym Sci 1961;2:465–95.
[4] Silberberg M, Supnik R. Tetrauoroethyene polymers. In: McCane DI, editor. Encyclopedia of Polymer Science and Technology, vol. 13. New York: Wiley; 1970. p. 623–54.
[5] Jones ED, Koo GP, O'Toole JL. A method for measuring compressive creep of thermoplastic materials. Mater Res Stand 1966;6:243–421.
[6] Jones ED, Koo GP, O'Toole JL. Time-dependent compressive properties of PTFE. Mod Plast 1967;137–40 see also pages 142, 192, 194, 198 and 202.
[7] Schulz AK. Sur la relaxation mechanique des matieres plastiques. Journal de Chimie Physique et de Physico-Chimie biologique 1956;53:933–8.
[8] Tobolsky AV, Katz D, Eisenberg A. Maximum relaxation times in polytetrafluoroethylene. J Appl Polym Sci 1963;7:469–74.
[9] Davies EDH, Hunter SC. The dynamic compression testing of solids by the method of the Split-Hopkinson pressure bar. J Mech Phys Solids 1963;11:155–79.
[10] Gray III GT, Cady CM, Blumenthal WR. Influence of temperature and strain rate on the constitutive behavior of Teflon and nylon. In: Kahn AS, editor. Plasticity 99: constitutive and damage modeling of inelastic deformation and phase transformation. Fulton, MD: Neat Press; 1998. p. 955–8.

[11] Walley SM, Field JE, Safford NA. A comparison of the high strain rate behaviour in compression of polymers at 300 and 100 K. J Phys IV Fr 1991;C3:185–90.
[12] Koo GP, Jones ED, Riddell MN, O'Toole JL. Engineering properties of a new polytetrafluoroethylene. Soc Plast J 1965;21(9):1100–5.
[13] DuPont-Fluoroproducts, Teflon, PTFE, properties handbook, Tech. Rep. H-37051-3, DuPont; 1996.
[14] Khan A, Zhang H. Finite deformation of a polymer: experiments and modeling. Int J Plast 2001;17:1167–88.
[15] Flack HD. High-pressure phase of polytetrafluoroethylene. J Polym Sci: Part A-2 1972;10:1799–809.
[16] Beecroft RI, Swenson CA. Behaviour of polytetrafluoroethylene (Teflon) under high pressures. J Appl Phys 1959;30(11):1793–8.
[17] Weir CE. Transitions and phases of polytetrafluoroethylene (Teflon). J Res Natl Bureau Stand 1953;50(2):95–7.
[18] Wu C-K, Nicol M. Raman spectra of high pressure phase and phase transition of polytetrafluoroethylene (Teflon). Chem Phys Lett 1973; 21(1):153–7.
[19] McCrum NG. An internal friction study of polytetrafluoroethylene. J Polym Sci 1959;34:355–69.
[20] Moynihan RE. The molecular structure of perfluorocarbon polymers. Infrared studies on polytetrafluoroethylene. J Am Chem Soc 1959;81: 1045–50.
[21] Lehnert RJ, Hendra PJ, Everall N, Clayden NJ. Comparative quantitative study on the crystallinity of poly(tetrafluoroethylene) including Raman, infrared and 19F nuclear magnetic resonance spectroscopy. Polymer 1997;38(7):1521–35.
[22] Ryland AL. X-ray diffraction. J Chem Educ 1958;35(2):80–3.
[23] Thomas PE, Londz JF, Sperati CA, McPherson JL. Effects on fabrication on the properties of Teflon resins. Soc Plast J 1956;12: 89–95.
[24] Walley SM, Field JE, Pope PH, Safford NA. A study of the rapid deformation behaviour of a range of polymers. Philos Trans R Soc London, A 1989;328:1–33.
[25] Walley SM, Field JE, Pope PH, Safford NA. The rapid deformation behaviour of various polymers. Journal de Physique III 1991;1(12): 1889–925.
[26] Gray III GT, Blumenthal WR. Split-Hopkinson pressure bar testing of soft materials. In: ASM-Handbook-Committee, editor. ASM handbook, mechanical testing and evaluation, vol. 8. ASM International; 2000.
[27] Panametrics, Ultrasonic technical notes, Tech. Rep., www.panametrics.com; 2001.
[28] Perepechko II, Sorokin VE. Velocity of ultrasound in polymers at liquid-helium temperatures. Sov Phys-Acoustics 1973;18(4):485–9.
[29] Marsh SP. LASL shock Hugioniot data. Berkeley, CA: University of California Press; 1980.
[30] Kaye GWC, Laby TH. Tables of physical and chemical constants, 16th ed. London: Longman; 1995.
[31] Kapoor R, Nemat-Nasser S. Determination of temperature rise during high-strain rate deformation. Mech Mater 1998;27:1–12.
[32] Rittel D. On the conversion of plastic work to heat during high strain rate deformation of glassy polymers. Mech Mater 1999;31:131–9.
[33] Furukawa GT, McCoskey RE, King GJ. Calorimetric properties of polytetrafluoroethylene (Teflon) from 0 to 365 K. J Res Natl Bureau Stand 1952;49(4):273–8.
[34] Ward IM. Mechanical properties of solid polymers, 2nd ed. New York: Wiley; 1979.
[35] Wortmann FJ. Analysing the relaxation behaviour of poly(tetrafluoroethylene) in the alpha-transition region by applying a two-component model. Polymer 1996;37(12):2471–6.
[36] Krum F, Muller H. Vorbehandlung und dielektrische verhalten Hochpolymerer. Kolloid-Zeitschrift 1959;162(2):81–107.
[37] Yosnio A. Thermal expansion coefficient of polttetrafluoroethylene in the vicinity of its glass transition at about 400 K. J Appl Polym Sci 1965;8:421–7.
[38] Woodward AE, Sauer JA. Mechanical relaxation phenomina. In: Fox D, editor. Physics and chemistry of the organic state. New York: Interscience; 1965. p. 637–723.
[39] Kvacheva LA, Perepechko II. Acoustical investigations of relaxation processes in polytetrafluoroethylene. Sov Phys-Acoustics 1973;18(3): 343–6.
[40] Lau SF, Suzuki H, Wunderlich B. The thermodynamic properties of polytetrafluoroethylene. J Polym Sci: Polym Phys Ed 1984;22: 379–405.